Available online at www.sciencedirect.com
ScienceDirect
Polymer 49 (2008) 561–569
polymer
www.elsevier.com/locate/polymer

Structural study of a series of ethylene–tetrafluoroethylene copolymers with various ethylene contents, Part 1: Structure at room temperature investigated for uniaxially-oriented samples by an organized combination of 2D-WAXD/SAXS and IR/Raman spectra

Suttinun Phongtamrug [a], Kohji Tashiro [a,*], Atsushi Funaki [b], Kiyotaka Arai [b], Shigeru Aida [b]

[a] *Department of Future Industry-oriented Basic Science and Materials, Toyota Technological Institute, Tempaku, Nagoya 468-8511, Japan*
[b] *Research and Development Division, Asahi Glass Co., Ltd., Yokohama, Kanagawa 221-8755, Japan*

Received 25 July 2007; received in revised form 10 November 2007; accepted 17 November 2007
Available online 21 November 2007

Abstract

The X-ray fiber diagrams, polarized infrared/Raman spectra, and small-angle X-ray scattering data have been successfully measured for a series of uniaxially-oriented ethylene (E)–tetrafluoroethylene (TFE) random copolymers. The difference in crystal structure and morphology has been investigated. All the samples of E/TFE copolymer were found to take the planar-zigzag conformation at room temperature except pure polytetrafluoroethylene case. The layer line intensities of the X-ray fiber diagram and the 00*l* reflection intensities were found to change systematically. From this, the E and TFE sequences were considered to be included commonly in a crystal lattice. The detailed investigation of the polarized infrared and Raman spectra allowed us to assign the bands to some characteristic structures. These can be used effectively in the study of structural changes occurring in the phase transition of these copolymer samples. The 2-dimensional small-angle X-ray scattering patterns were compared among the copolymers and the difference in stacked lamellar structure has been discussed.

Keywords: Ethylene–tetrafluoroethylene copolymer; X-ray diffraction; Vibrational spectra

1. Introduction

When the different types of monomeric units are combined together to give a copolymer, we may have a new polymer with superior mechanical or chemical properties from the original homopolymers. We will focus here a series of random copolymers consisting of ethylene (E) and tetrafluoroethylene (TFE) monomeric units. The most popular member is an E/TFE copolymer with E (and TFE) content of about 50 mol% containing a small amount of an additive which is needed for industrial purposes such as enhancement of processability, etc. This copolymer is commercially available with the trade names Tefzel of DuPont, Fluon of Asahi Glass Co., Ltd., and Texlon of Vector Foiltec and applied in a wide field due to its high transparency, high weatherability, and thermal stability in addition to mechanical strength [1]. What happens in the physicochemical properties if the relative content of E and TFE monomeric units is modified from 50 mol%? To answer this question, it is important to understand the behavior of a series of E/TFE copolymers from the structural point of view, in particular, the characteristic features of the crystal structure as well as the higher order structure. So far several reports have been published on the crystal structures of E/TFE copolymer on the basis of X-ray diffraction profiles [2–6]. Unfortunately, the samples used in these studies were mostly the unoriented form so the several

* Corresponding author. Tel.: +81 52 809 1790; fax: +81 52 809 1793.
E-mail address: ktashiro@toyota-ti.ac.jp (K. Tashiro).

0032-3861/$ - see front matter © 2007 Elsevier Ltd. All rights reserved.
doi:10.1016/j.polymer.2007.11.036

reflections coming from both the equatorial and layer lines were overlapped, thus making it difficult to discuss the structural features unambiguously. Therefore, it would be more useful to make a detailed analysis of the structure of uniaxially-oriented samples consisting of only the two kinds of monomers without any third component. For example, in Ref. [7] the X-ray fiber diagram of 50/50 E/TFE copolymer was used for the structural analysis of the crystal lattice, but the sample contained a small amount of third component. In Refs. [8,9] the polarized infrared and Raman spectral data were measured to assign vibrational bands by combining them with the normal coordinates treatments, but the characterization of the monomer ratio was not clear. However, in these researches the uniaxially-oriented samples were used, which helped us to understand the structural features of this copolymer. But, strictly speaking, the sample reported as the 50/50 E/TFE copolymer was not a pure copolymer consisting only of 50/50 E/TFE monomeric units as pointed out already. We speculate that it contained a small amount of additive, which makes the structural discussion more complicated because the crystallization behavior is sensitive to a third component [3,6,10,11].

In the present study, we have synthesized a series of E/TFE copolymers consisting of the various molar ratios of E and TFE monomeric units without any third component. We prepared the uniaxially-oriented samples so that the change in crystal structure can be clarified in detail on the basis of 2-dimensional X-ray diffraction diagram and polarized infrared and Raman spectra. Additionally, the small-angle X-ray scattering has been also measured to clarify the effect of E/TFE content on the stacking structure of lamellae. These E/TFE copolymers were found to show the phase transitions between low- and high-temperature phases in the heating/cooling process [3,4,6,12,13]. Information on the structural changes in the phase transitions is quite important to reveal the essential features of these copolymers. The details of the phase transition behaviors will be reported in a separate paper. The present paper reports our attempt to compare the crystal structure among a series of E/TFE copolymers at room temperature.

2. Experimental

2.1. Samples

A series of E/TFE copolymers were synthesized by a radical polymerization reaction in the perfluoropentyl difluoromethane solution. The chemical composition was analyzed by the molten-state ^{19}F NMR measurement and the fluorine ultimate elementary analysis. The monomer contents of these copolymers were as follows: E/TFE = 100/0 (polyethylene, PE), 61/39, 50/50, 35/65, 29/71, and 0/100 mol% (polytetrafluoroethylene, PTFE).

The samples were molten and quenched into ice-water bath, followed by stretching about 3 times the original length at about 100 °C and then annealed at about 20 °C below the melting temperature for 3 h under tension, where the melting temperature measured by DSC was 232 °C for E/TFE 61/39, 280 °C for 50/50, 250 °C for 35/65, and 251 °C for 29/71 samples. The thus prepared uniaxially-oriented samples with ca. 0.3 mm thickness were used for the X-ray diffraction measurements as well as the Raman spectral measurements. Oriented thin films of ca. 20 μm thickness were used for the infrared spectral measurements.

2.2. Measurements

The X-ray fiber diagrams were measured at room temperature using a MAC Science DIP1000 X-ray diffraction system with a graphite-monochromatized Mo Kα line ($\lambda =$ 0.71073 Å) as an incident X-ray beam. An imaging plate was used as a 2-dimensional detector which was installed in the DIP1000 system. The Weissenberg photographs were measured with a Norman method using a cylindrical camera of 28.65 mm radius, where the oriented samples were rotated around the axis perpendicular to the draw direction to measure the meridional 00*l* reflections. An imaging plate was set on the cylindrical camera to record the diffraction patterns. The 2-dimensional small-angle X-ray scattering (SAXS) patterns were measured using a Rigaku Nanoviewer with an X-ray beam of Cu Kα line which was finely focused by a confocal mirror. The SAXS patterns were recorded at room temperature on the imaging plate at a sample-to-plate distance of ca. 70 cm. The polarized Raman spectra were measured using a Japan Spectroscopic Company NRS-2100 laser Raman spectrophotometer at the back-scattering geometry with an exciting laser beam of 532 nm. Three different polarization geometries, $X(ZZ)X$, $X(YZ)X$ and $X(YY)X$, were used at room temperature on the Cartesian coordinates system *XYZ*, where the *Z* axis was parallel to the draw axis and the *X* and *Y* axes were perpendicular to the *Z* axis. The $X(YZ)X$ symbol represents the scattering geometry based on the Porto's symbol [14]: the laser beam with an electric vector E_Y is incident to the sample along the *X* direction and the scattered beam with an electric vector E_Z is detected in the *X* direction. The polarized infrared spectra were measured at room temperature with a Varian FTS-7000 Fourier-transform infrared spectrometer equipped with a wire-grid polarizer. The resolution power for the Raman and infrared measurements was 2 cm^{-1}.

3. Results and discussion

3.1. X-ray diffraction patterns

Fig. 1 shows the X-ray fiber diagrams taken at room temperature for a series of uniaxially-oriented E/TFE copolymer samples including PE and PTFE. Fig. 2 shows the Weissenberg photographs developed for the meridional 00*l* reflections.

In Fig. 1 the layer lines can be counted as 0th (equatorial), 1st, 2nd, 3rd, and 4th lines for E/TFE 50/50 copolymer. The interlayer spacings give the fiber period of 5.10 Å for all the samples except PE and PTFE. The 00*l* reflections observed in Weissenberg photograph of 50/50 E/TFE copolymer sample gave a fiber period consistent with this value. Therefore, the chain conformation of E/TFE copolymers is of the *trans*-zigzag form [2,7,8].

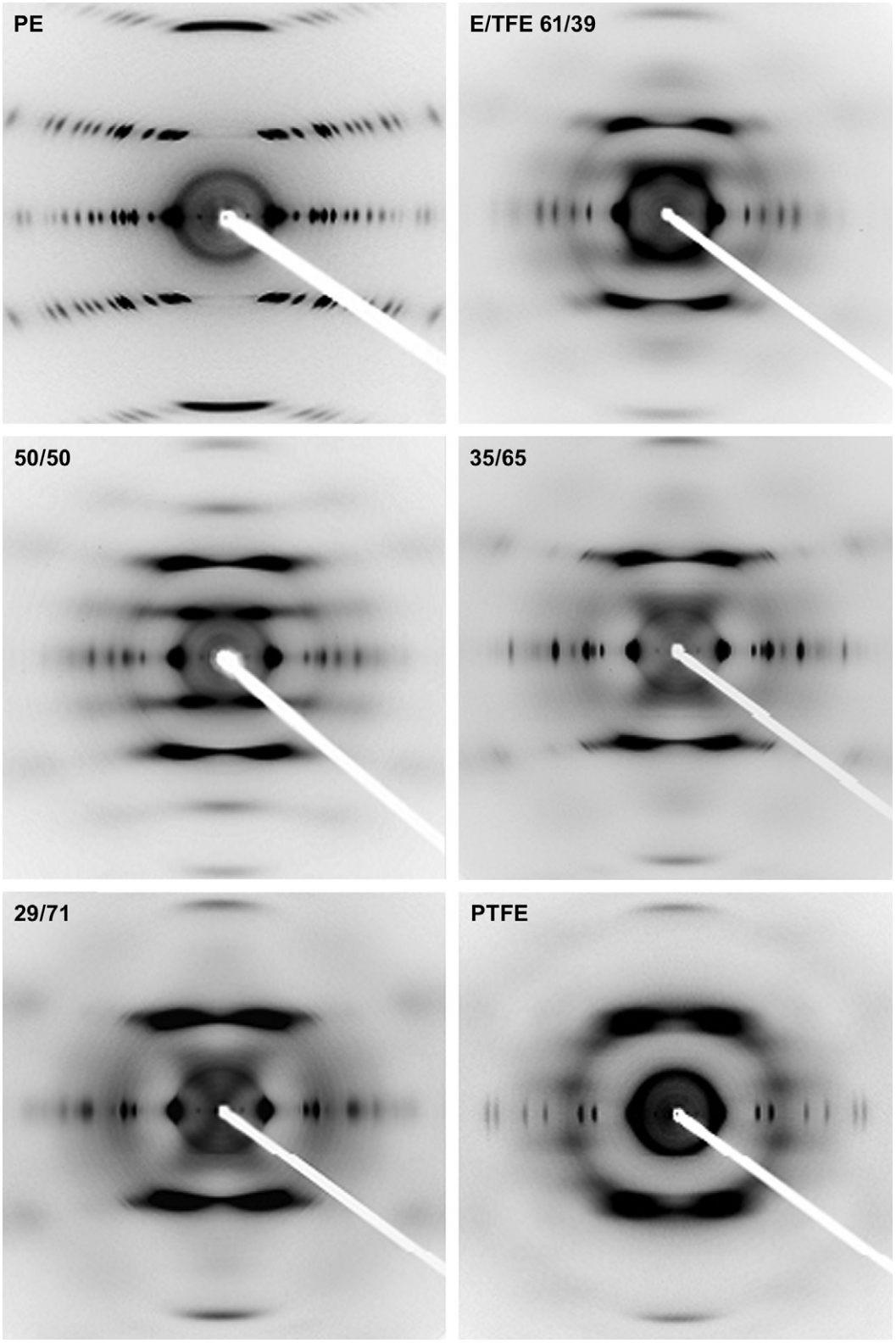

Fig. 1. X-ray fiber diagrams taken for a series of uniaxially-oriented E/TFE copolymer samples at room temperature. The incident X-ray beam was Mo Kα.

As the E/TFE ratio changes to 61/39, 35/65, and 29/71, the 1st and 3rd layer lines observed for E/TFE 50/50 copolymer become weaker and more diffuse before finally almost disappearing as seen in Fig. 1. This observation can be confirmed by taking the Weissenberg photographs as shown in Fig. 2. If we ignore completely these weak reflections, then apparent fiber period is ca. 2.55 Å for E/TFE 35/65 and 29/71 samples. The fiber period changes gradually from 2.55 Å to 5.10 Å as

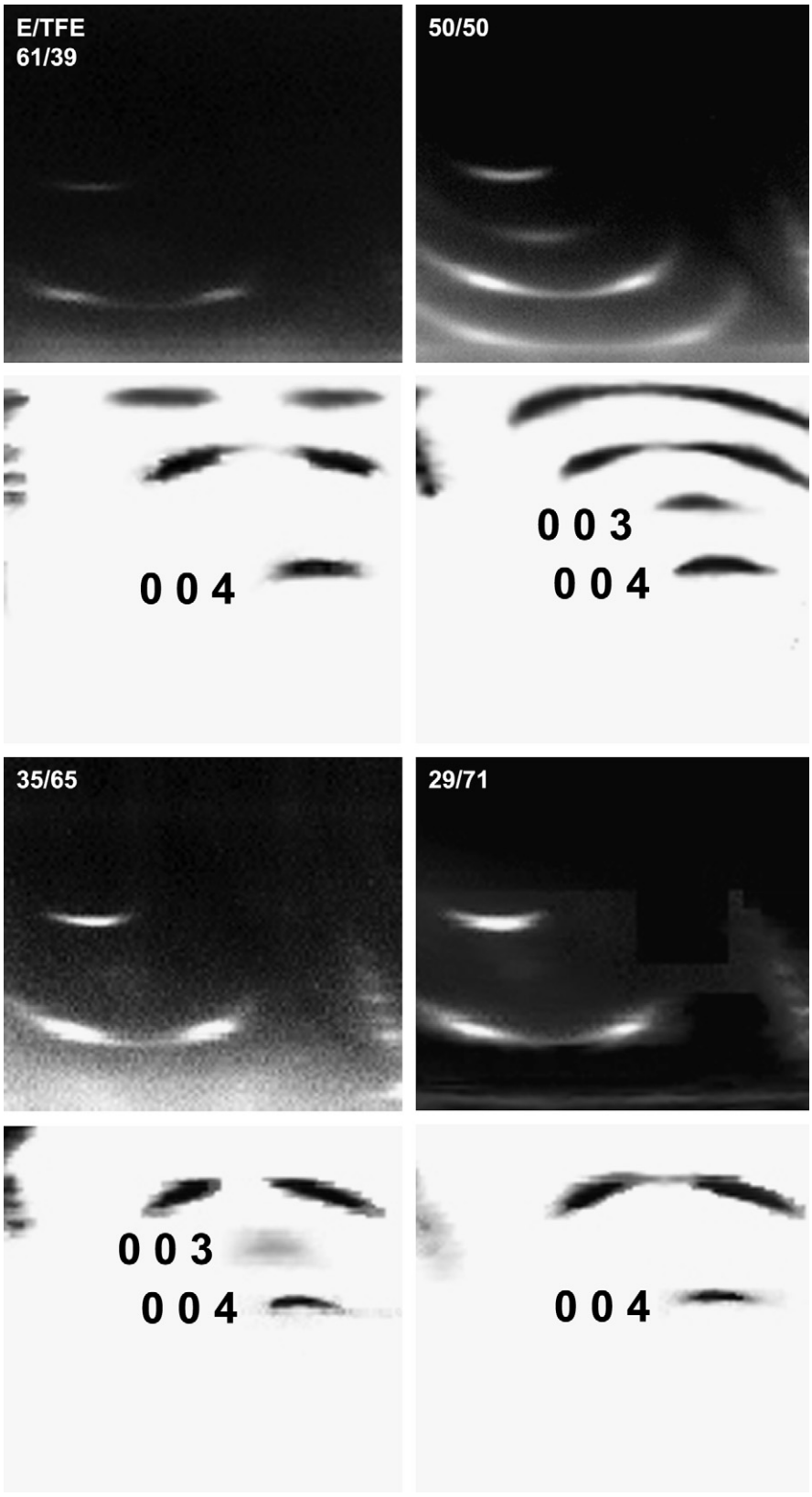

Fig. 2. Weissenberg photographs taken for a series of uniaxially-oriented E/TFE copolymer samples at room temperature by Norman method to detect the 00*l* reflections.

the ethylene content is changed from 29 to 61 mol%. However, the fiber period of pure PE reverts to 2.55 Å [15]. These observations can be interpreted reasonably as illustrated in Fig. 3.

Alternation of E and TFE monomeric units, which can be realized typically for E/TFE 50/50 copolymer, disappears gradually as the E or TFE monomer content begins to overwhelm the TFE or E content, respectively. Correspondingly, the averaged fiber period changes as shown in Fig. 3. PTFE itself does not take the perfect planar-zigzag conformation but the helical conformation with slightly contracted period (16.88 Å for 13/6 helix and 19.50 Å for 15/7 helix) [16–19]. However, as in the case of vinylidene fluoride–tetrafluoroethylene copolymers [20,21], the TFE segments included in the copolymer chains are considered to take essentially the planar-zigzag conformation as long as the TFE segmental length is not very long. This is different from PTFE homopolymer. Corresponding to the changes in layer line intensity given in Fig. 1, the 00*l* reflections change the intensity also as seen in Fig. 2. This observation can be understood reasonably by deriving the structure factor of 00*l* reflection, $F(00l)$. Referring to the models shown in Fig. 3, $F(00l)$ is expressed as below.

For the alternating sequence of E and TFE monomeric units:

$$F_{\mathrm{E/TFE}}(00l) = \sum_j f_j \exp\left(2\pi i z_j l\right) = f(\mathrm{E})[1+\exp(\pi i l/2)] + f(\mathrm{TFE})[\exp(\pi i l) + \exp(3\pi i l/2)] \quad (1)$$

For the homopolymers:

$$\mathrm{PE}: \quad F_{\mathrm{PE}}(00l) = f(\mathrm{E})[1+\exp(\pi i l/2)+\exp(\pi i l) + \exp(3\pi i l/2)] \quad (2-1)$$

$$\mathrm{PTFE}: \quad F_{\mathrm{PTFE}}(00l) = f(\mathrm{TFE})[1+\exp(\pi i l/2)+\exp(\pi i l) + \exp(3\pi i l/2)] \quad (2-2)$$

where f(E) and f(TFE) are structure factors of ethylene and tetrafluoroethylene units, respectively. In these equations the planar-zigzag conformation is assumed for both of PE and PTFE and the fiber period is assumed to be twice the original values so as to compare the intensity change of 00*l* reflection with that of E/TFE copolymer. If the E and TFE monomeric units are arranged randomly along the chain axis, then we will have the averaged structure factor F(00*l*) as:

$$1 \geq X \geq 0.5 \quad F(00l) = \left[(1-X)\times F_{\mathrm{E/TFE}}(00l) + (2X-1)\times F_{\mathrm{PE}}(00l)\right]/X \quad (3)$$

$$0 \leq X \leq 0.5 \quad F(00l) = \left[(X)\times F_{\mathrm{E/TFE}}(00l) + (1-2X)\times F_{\mathrm{PTFE}}(00l)\right]/(1-X) \quad (4)$$

where the content of E monomeric unit is assumed to be X. By substituting Eqs. (1) and (2) into Eqs. (3) and (4), we have the diffraction intensity $I(00l)$ as shown in Table 1, which is proportional to the square of structure factor: $I(00l) \propto F(00l)F^*(00l)$ where F^* is a conjugate of F. Since the electron density of TFE unit is much higher than that of E unit, f(E) − f(TFE) is far from zero. As a result, the 00*1* and 00*3* reflections are relatively weaker, the 00*2* reflection does not show any intensity, and the 00*4* reflection is the strongest. This is consistent with the observed results from Fig. 2. It should be noted here that the 00*4* reflection for $X = 0$ and 1 is the 00*2* reflection for PTFE and PE, respectively, as long as the planar-zigzag conformation is assumed. As the E content (or TFE content) is deviated from 0.5, the relative intensity of 00*l* is changed. The similar situation can be also observed for the relative intensity of the layer lines. From these interpretations, we may say that the E, TFE, and E/TFE segments are included commonly in a crystallite to cause the coherent X-ray diffraction. In other words, these segments are cocrystallized together in a common lattice.

Fig. 4 shows the X-ray equatorial profiles derived from Fig. 1. The innermost reflection at ca. 8° (for Mo Kα line) and the neighboring reflection at ca. 9° are tentatively indexed, respectively, as 120 and 200 of the orthorhombic unit cell proposed for E/TFE 50/50 copolymer although the sample used in the paper contained a small amount of the third (and forth) component [7]. For E/TFE 35/65 and 29/71 copolymer samples, the reflection at ca. 8° is apparently a singlet at room temperature, but it splits into two at such a low temperature (−50 °C) [22]. Therefore, an orthorhombic unit cell model cannot be applied to these two copolymers. Rather, a monoclinic unit cell might be suitable for them. The details will be reported in a separate paper after a more complete structure analysis based on the X-ray diagrams shown in Fig. 1.

Although we do not report here the temperature dependence of X-ray diffraction profile, it may be worthwhile to

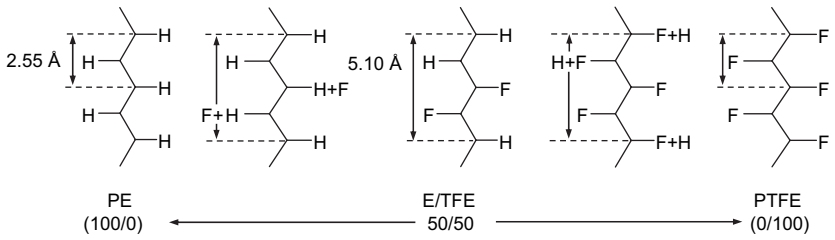

Fig. 3. Planar-zigzag chain models illustrated for a series of E/TFE copolymers.

Table 1
Relative intensity of the 00*l* reflections derived for E/TFE copolymers[a]

$I(00l)$[b]					
	E/TFE ($X=0.5$)	PE ($X=1$)	PTFE ($X=0$)	E/TFE	
$l=1$	$[f(\mathrm{E})-f(\mathrm{TFE})]^2$	0	0	$1\geq X\geq 0.5$	$[(1-X)/X]^2[f(\mathrm{E})-f(\mathrm{TFE})]^2$
				$0\leq X\leq 0.5$	$[X/(1-X)]^2[f(\mathrm{E})-f(\mathrm{TFE})]^2$
$l=2$	0	0	0	0	
$l=3$	$[f(\mathrm{E})-f(\mathrm{TFE})]^2$	0	0	$1\geq X\geq 0.5$	$[(1-X)/X]^2[f(\mathrm{E})-f(\mathrm{TFE})]^2$
				$0\leq X\leq 0.5$	$[X/(1-X)]^2[f(\mathrm{E})-f(\mathrm{TFE})]^2$
$l=4$	$[f(\mathrm{E})+f(\mathrm{TFE})]^2$	$f(\mathrm{E})^2$	$f(\mathrm{TFE})^2$	$1\geq X\geq 0.5$	$\{[(3X-1)f(\mathrm{E})+(1-X)f(\mathrm{TFE})]/X\}^2$
				$0\leq X\leq 0.5$	$\{[Xf(\mathrm{E})+(2-3X)f(\mathrm{TFE})]/(1-X)\}^2$

[a] $f(\mathrm{E})$ and $f(\mathrm{TFE})$ are the structure factors of ethylene ($-CH_2CH_2-$) and tetrafluoroethylene ($-CF_2CF_2-$) units, respectively. X is the molar content of ethylene monomeric unit.
[b] $I(00l)$ is the relative intensity, where the proportional coefficients are neglected for simplicity.

point out that the innermost two reflections of the equatorial line merge into a sharp and intense singlet in higher temperature region [3,4,6,13,22,23]. That is, the apparently orthorhombic unit cell change to the pseudo-hexagonal lattice. At higher temperature, the molecular chains rotate around the chain axis. However, this is not a simple rotation of rigid *trans*-zigzag chains but is a combination of rotational motion with *trans*-to-*gauche* conformational exchange occurring partially along the skeletal chain. This is confirmed by the infrared and Raman spectral measurements made at high temperature [12,23,24]. The behavior varies depending on the E/TFE relative ratio.

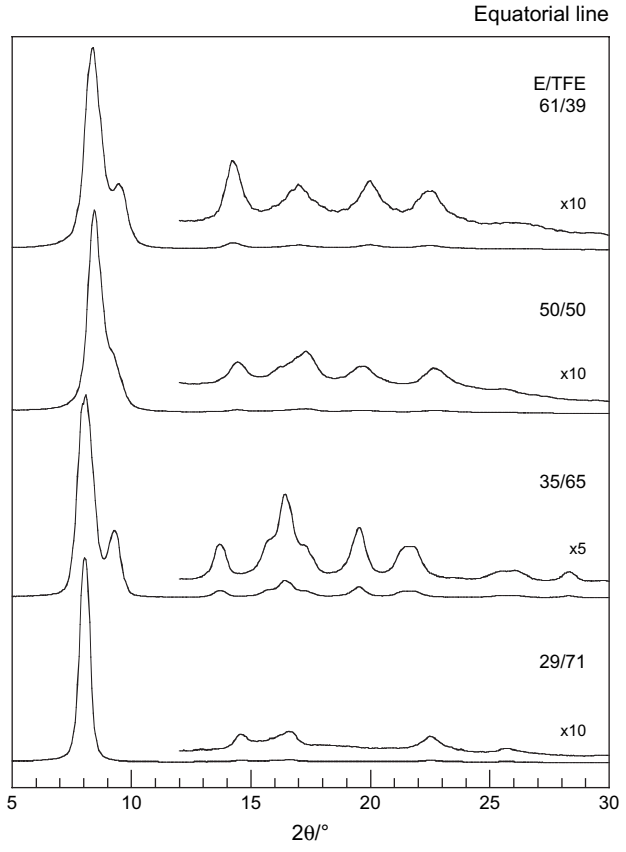

Fig. 4. X-ray equatorial diffraction profiles derived from Fig. 1 for a series of E/TFE copolymers.

3.2. Polarized infrared and Raman spectra

Fig. 5 shows the polarized infrared spectra measured at room temperature for a series of oriented E/TFE copolymer samples. The solid and broken lines correspond, respectively, to the spectra taken with an electric vector of incident infrared beam perpendicular and parallel to the draw direction of the sample. In this figure the spectra of PE, PTFE, and poly(vinylidene fluoride) (PVDF) form I are also included, where PE and PVDF form I take the planar-zigzag chain conformation [25,26] but the helical conformation for PTFE. Fig. 6 shows the polarized Raman spectra of all these polymer samples, where the *ZZ* and *YZ* components are included. The *Z* axis is defined as the axis parallel to the draw direction. The *Y* axis is perpendicular to the *Z* axis. By comparing these spectra with those of PE, PTFE, and PVDF form I, we can assign the several typical bands to various types of segments.

3.2.1. Characteristic Raman bands

For example, in Fig. 6(a), the bands at around 840 cm^{-1} are not observed for both PE and PTFE but rather correspond to the CF_2 stretching mode of CH_2CF_2 sequence as detected for PVDF form I [8,27]. The band at about 730 cm^{-1} is strong for PTFE and decreases in intensity as the TFE content is decreased and disappears almost at 50 mol% content, where the polymer is an almost perfectly alternating copolymer and the CF_2CF_2 segment is isolated by being sandwiched by CH_2CH_2 units. Therefore the 730 cm^{-1} band is considered to originate from the TFE sequence longer than $CF_2CF_2CF_2CF_2$ of *trans* form. A pair of bands at 1400–1450 cm^{-1} was assigned by Rabolt et al. to a correlation splitting coming from the ethylene *trans*-zigzag chains packed in an orthorhombic (or herringbone) mode from Raman spectra of E/TFE 50/50 copolymer [9]. These bands are observed commonly to all the E/TFE copolymers and they are quite sharp and most intense. Since the probability of the CH_2CH_2 units encountering the other CH_2CH_2 units belonging to the neighboring chains is low for the copolymer of low E content, it is difficult to say that they come from the correlation splitting in the orthorhombic lattice. Rather they may be assigned to the local CH_2CH_2 sequential modes [28] and are not sensitive to the segmental length. Although the data are not shown

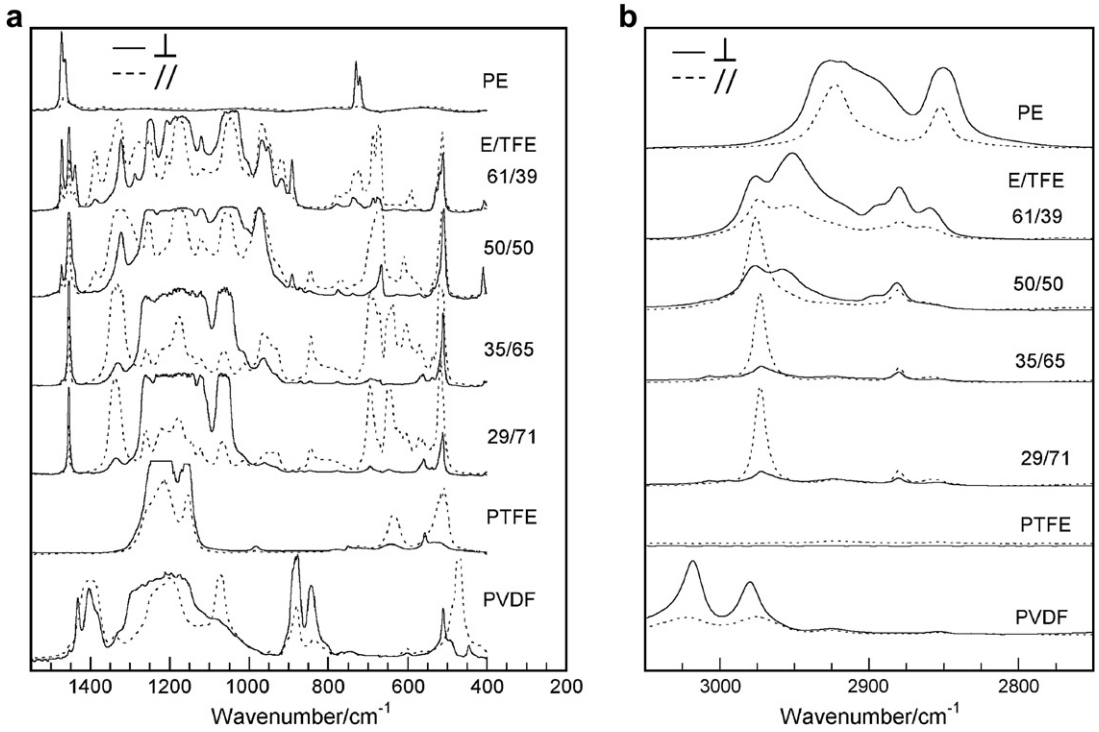

Fig. 5. Polarized infrared spectra taken at room temperature for a series of oriented E/TFE copolymer samples in the region of (a) 400–1550 cm^{-1} and (b) 2750–3050 cm^{-1}. The solid and broken lines represent, respectively, the spectral components measured with an electric vector of incident infrared beam perpendicular and parallel to the orientation axis.

here, the half-width of this sharp 1442 cm^{-1} band becomes broader in a phase transition temperature region, where the molecular chains start to rotate around the chain axis [12,23]. Therefore the 1442 cm^{-1} band seems to be sensitive to the thermal motion of the CH_2CH_2 chain segments. This knowledge will be useful for the discussion of structural features observed in the phase transition phenomenon of E/TFE copolymers. The bands at around 1000–1100 cm^{-1} are assignable to the CC skeletal stretching modes, and the spectral profiles change depending on the E content.

The spectral profile in the region of 2850–3000 cm^{-1} is quite complicated (Fig. 6(b)). The CH_2 stretching modes

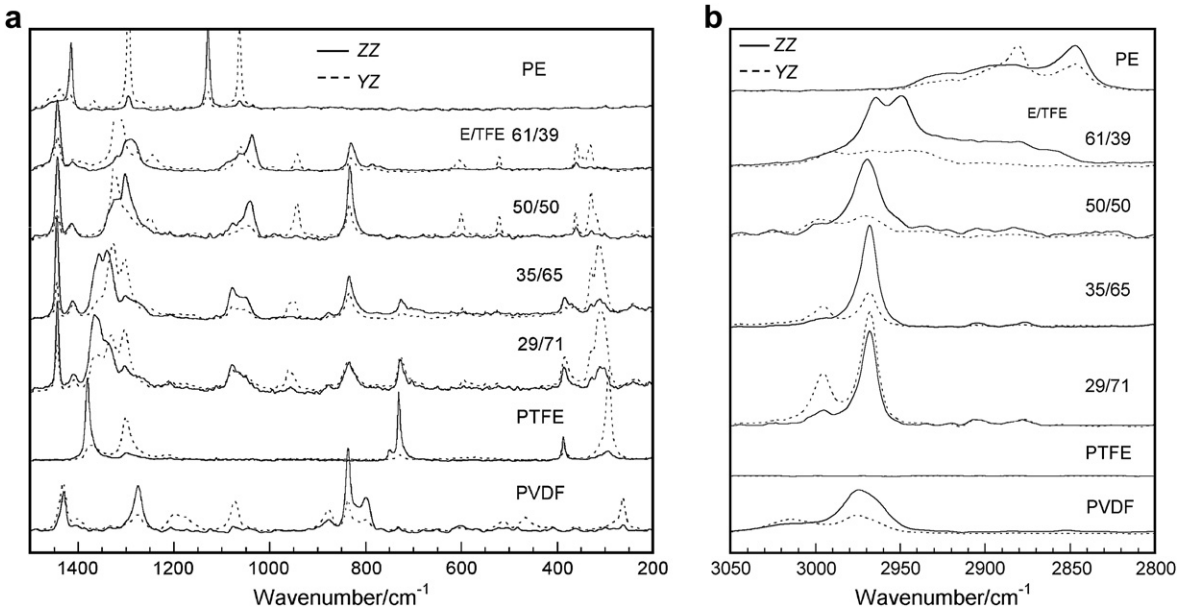

Fig. 6. Polarized Raman spectra taken at room temperature for a series of oriented E/TFE copolymer samples in the region of (a) 200–1500 cm^{-1} and (b) 2800–3050 cm^{-1}. The solid and broken lines represent the *ZZ* and *YZ* components, respectively. The *Z* axis is parallel to the orientation direction and the *Y* axis is perpendicular to the *Z* axis.

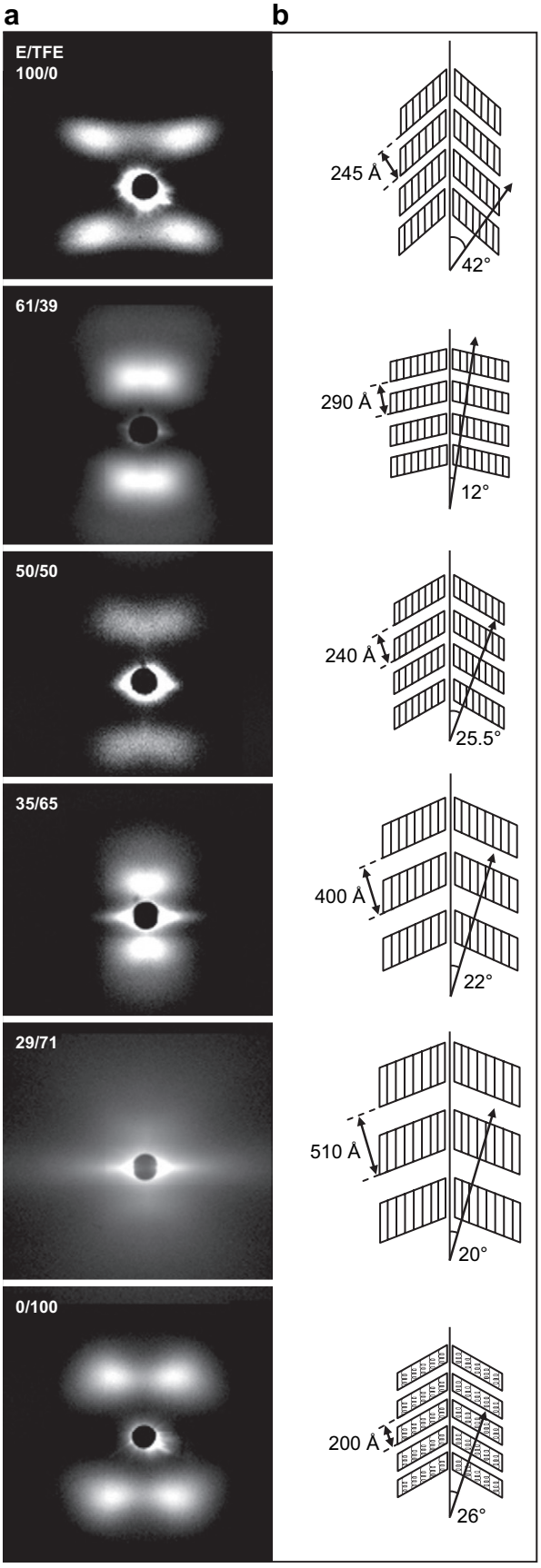

Fig. 7. (a) Small-angle X-ray scattering patterns measured at room temperature for a series of uniaxially-oriented E/TFE copolymer samples. The vertical axis is parallel to the draw direction. (b) Schematic illustrations of lamellar stacking structure for a series of E/TFE copolymer samples.

appear normally at around 2850–2900 cm^{-1} as typically seen for PE, but the corresponding bands are weak for E/TFE 61/39 copolymer. A sharp band is detected at about 2975 cm^{-1}, which shifts toward lower frequency region for the copolymer with higher E content. As being discussed for the Raman band profile of PE [29], the complicated profile might be interpreted in terms of Fermi resonance or the vibrational coupling between the normal CH_2 modes and the overtones of CH_2 scissoring mode located in the 1450 cm^{-1} region.

3.2.2. Characteristic infrared bands

As shown in Fig. 5(a), the band profile in 1450 cm^{-1} region can be assigned similarly to the Raman bands. A perpendicularly-polarized sharp 1450 cm^{-1} band is considered to come from the local CH_2 scissoring mode which is not very sensitive to any change in environment. However, the band profile splits into two as the E content approaches pure PE. They might come from the correlation splitting, which is not detected clearly in the Raman spectra as discussed above. The relative intensity of these bands is found to decrease above the transition temperature from orthorhombic to pseudo-hexagonal unit cell, though the data are not presented in this paper [24]. The band observed at 2975 cm^{-1} (Fig. 5(b)), which is detected also in Raman spectra, shows a parallel polarization and common to the E/TFE copolymers of E 39–71 mol%, cannot be assigned to the CH_2 local stretching mode because it should show a perpendicular polarization normally for the planar-zigzag chain. The bands at 2850–2900 cm^{-1} might be assignable to CH_2 stretching modes, since they increase in intensity for E-richer copolymer. The infrared bands at 510 cm^{-1} (∥), 600–700 cm^{-1} (∥), and 840 cm^{-1} (∥) are commonly observed with relatively strong intensity for E/TFE 29/71–50/50 samples and they start to decrease in intensity for E/TFE 61/39 copolymer. Since the CF_2 groups have larger electric dipole moments than CH_2 groups, the vibrational bands of CF_2 groups are considered to give much higher absorption intensity. Therefore, they are considered to originate from the vibrational modes characteristic of CF_2 segments. The bands at 900 cm^{-1} (⊥) and 1380 cm^{-1} (∥) come from E segments since they become stronger for E-richer copolymer samples.

In this way, there are various types of infrared and Raman bands which should be useful for the qualitative (even quantitative) interpretation of structural changes observed in the phase transition phenomena in terms of regular segmental length, intermolecular correlation, thermal mobility and so on. We need to confirm these tentative and qualitative assignments definitely by performing the normal coordinates treatment with intermolecular interactions taken into account.

3.3. Small-angle X-ray scatterings

Fig. 7(a) shows the 2-dimensional SAXS profiles taken for a series of uniaxially-oriented E/TFE copolymers at room temperature. Common features are as follows: (i) the four-point scattering patterns are observed for all the samples; from this the tilting angle of stacked lamellae is estimated to be approximately 12° (E/TFE 61/39) to 26° (E/TFE 50/50 to PTFE), although the scattering pattern becomes diffuse for E/TFE 29/71 sample, and (ii) the long period estimated is not systematic but changes between 200 Å and 500 Å, which may be affected by slight differences in such sample preparation conditions as the stretching ratio, the stretching temperature, the annealing temperature, etc. The schematic illustration of lamellar stacking structure is given in Fig. 7(b).

4. Conclusions

In the present paper we compared the structural features extracted from the characteristic patterns of X-ray fiber diagrams and Weissenberg photographs measured for a series of E/TFE copolymers using uniaxially-oriented samples rather than the previously studied unoriented ones. We have been able to clarify the systematic change of structure because the equatorial and layer line reflections are separated unambiguously. The systematic change in 00*l* reflection intensity can be interpreted reasonably on the basis of random distribution of E and TFE monomeric units along the chain axis. It is doubtful that the copolymers with higher TFE content form an orthorhombic unit cell, instead a monoclinic unit cell form is proposed because the innermost reflection is found to split into two at lower temperature. This will be reported in more detail elsewhere.

The detailed comparison of a series of polarized infrared and Raman spectral profiles has allowed us to assign some bands to characteristic structural features. It is possible to use these characteristic bands in the discussion of phase transition phenomena from the viewpoints of thermal motion, correlation of neighboring chain segments, regular sequence of monomeric units, etc. A full description of the structural changes in the phase transitions of a series of E/TFE copolymer samples will be reported in a future paper.

Acknowledgment

This work was financially supported by MEXT ‘‘Collaboration with Local Communities’’ Project (2005–2009).

References

[1] Drobny J. Rapra Rev Rep 2006;16:184.
[2] Wilson FC, Starkweather Jr HW. J Polym Sci Part A-2 1973;11:919–27.
[3] Pieper T, Heise B, Wilke W. Polymer 1989;30:1768–75.
[4] Iuliano M, De Rosa C, Guerra G, Petraccone V, Corradini P. Makromol Chem 1989;190:827–35.
[5] Petraccone V, De Rosa C, Guerra G, Iuliano M, Corradini P. Polymer 1992;33:22–6.
[6] D’Aniello C, De Rosa C, Guerra G, Petraccone V, Corradini P, Ajroldi G. Polymer 1995;36:967–73.
[7] Tanigami T, Yamaura K, Matsuzawa S, Ishikawa M, Mizoguchi K, Miyasaka K. Polymer 1986;27:999–1006.
[8] Kobayashi M, Tashiro K, Tadokoro H. Macromolecules 1975;8:158–71.
[9] Zabel K, Schlotter NE, Rabolt JF. Macromolecules 1983;16:446–52.
[10] De Rosa C, Guerra G, D’Aniello C, Petraccone V, Corradini P, Ajroldi G. J Appl Polym Sci 1995;56:271–8.
[11] Funaki A, Arai K, Aida S, Tashiro K. Polym Prepr Jpn 2006;55:3514.
[12] Tashiro K, Kobayashi M. Polym Prepr Jpn 1987;36:2339–41.
[13] Tanigami T, Yamaura K, Matsuzawa S, Ishikawa M, Mizoguchi K, Miyasaka K. Polymer 1986;27:1521–8.
[14] Damen TC, Porto SPS, Tell B. Phys Rev 1966;142:570–4.
[15] Bunn CW. Trans Faraday Soc 1939;35:482–91.
[16] Bunn CW, Howells ER. Nature 1954;174:549–51.
[17] Sperati CA, Starkweather Jr HW. Adv Polym Sci 1961;2:465–95.
[18] Clark ES, Muus LT. Z Kristallogr 1962;117:119–27.
[19] Weeks JJ, Clark ES, Eby RK. Polymer 1981;22:1480–6.
[20] Tashiro K, Kaito H, Kobayashi M. Polymer 1992;33:2915–28.
[21] Tashiro K, Kaito H, Kobayashi M. Polymer 1992;33:2929–33.
[22] Phongtamrug S, Tashiro K, Funaki A, Arai K, Aida S. Polym Prepr Jpn 2007;56:717.
[23] Phongtamrug S, Tashiro K, Funaki A, Arai K, Aida S. Macromol Symp 2006;242:268–73.
[24] Phongtamrug S, Tashiro K, Funaki A, Arai K, Aida S. Polym Prepr Jpn 2006;55:3560.
[25] Lando JB, Olf HG, Peterlin A. J Polym Sci Part A-1 1966;4:941–51.
[26] Hasegawa R, Takahashi Y, Chatani Y, Tadokoro H. Polym J 1972;3:600–10.
[27] Tashiro K, Itoh Y, Kobayashi M, Tadokoro H. Macromolecules 1985;18:2600–6.
[28] Radice S, Del Fanti N, Zerbi G. Polymer 1997;38:2753–8.
[29] Snyder RG, Hsu SL, Krimm S. Spectrochim Acta 1978;34A:395–406.